JCE

Journal of Civil Engineering
ISSN 2086 - 1206 E-ISSN 2579 - 9029

Behaviour of RC Beam-Slab Member with Embedded Polystyrene Spheres

Jen Hua Ling[a]*, Ji Wei Lau[a], Yong Tat Lim[a]

Correspondence

[a]Centre for Research of Innovation & Sustainable Development, School of Engineering and Technology, University of Technology Sarawak, 96000 Sibu, Sarawak, Malaysia.

Corresponding author email address: lingjenhua@uts.edu.my

Submitted : 01 January 2024
Revised : 03 February 2025
Accepted : 18 February 2025

Abstract

In this study, four reinforced concrete specimens were produced. Each specimen consisted of two beams and one slab. Polystyrene spheres were used to replace concrete in the beams and slabs in various combinations to reduce weight. The specimens were subjected to an incremental static load under the four-point load setup. The effects of polystyrene spheres on the structural performance of these specimens were investigated. The specimen with solid beams and lightweight slab (i.e., embedded with polystyrene spheres) had the highest material efficiency. Its efficiency was 5% higher than that of the entirely solid specimen. The material's effectiveness decreased by 2% to 4% when the beams were filled with polystyrene spheres. This was regardless of whether the slab contained polystyrene spheres. From feasibility analysis, none of the specimens fulfilled all five assessment criteria. Ductility was a concern for the specimens. The current specimen designs were unable to outstrength the solid specimen. The size and shape of the polystyrene, as well as the dimension of the specimen, may be modified to improve its efficiency.

Keywords

Reinforced concrete, beam-slab system, polystyrene spheres, flexural behaviour, four-point load test

INTRODUCTION

Reinforced concrete (RC) structures are popular due to their stability, ductility, and material availability [1]. One issue with RC structures is their low strength-to-weight ratio [2]. The weight imposes extra loads on the columns and foundations, leading to larger sections [3].

One way of reducing the weight of an RC member is to embed lightweight materials in it. The lightweight materials create voids in the member and change its sectional properties. This subsequently affects the member's structural performance. Concrete removal can reduce a member's stiffness, load capacity, and ductility [4] – [6]. It also quickens the formation and growth of cracks [3], [7] and reduces the shear resistance of the member [8]. Nonetheless, by incorporating lightweight materials, concrete's efficiency can be increased [9], [10].

To reduce the negative effects on the member's performance, lightweight materials should be strategically placed, concrete removal should be limited, and appropriate shapes should be used. Lightweight materials were suggested to be placed in the tension zone of a bending member, which is the low-stressed zone [11]. In previous studies, the concrete replacement in beams and slabs barely exceeded 20% and 30% respectively [12]. Sharp edges and pointed corners should be avoided to prevent stress concentration in the member [9], [13], [14].

Table 1 summarises previous studies on reducing the weight of RC members. There were two methods identified: creating voids or embedding lightweight materials. These materials were larger than the aggregates used in the concrete mix [12]. Some common shapes were spheres, cubes, and ellipsoids. There have been studies on individual beams and slabs, but none on beam-and-slab systems.

In this study, polystyrene spheres were used as lightweight materials to be embedded in RC members comprising beams and slabs. The members' behaviour and the effects of polystyrene spheres were investigated. The members were later evaluated for feasibility based on a set of criteria.

Table 1: Materials used to reduce the weight of RC members

Methods	Beam	Slab
Creating voids in a member	PVC pipe [15] - [23]	High-density polyethylene (HDPE) [24] - [26]
	Plastic ball or void former [27] - [31]	Plastic [32] - [37]
	Plastic bottle [38], [39]	Glass fiber plastic [32]
	Seeding tray [40]	recycled plastic [34], [41] Paper tube [42]
Embedding lightweight in a member	Polystyrene spheres [4], [43]	Styropor / polystyrene [7], [12], [33], [44], [45]

Table 1: Materials used to reduce the weight of RC members

Methods	Beam	Slab
	Polystyrene block [10], [13], [46], [47]	Industrial sponge [48]
	Foamed concrete infill [49]	
	Polypropylene Plastic Sheet [50]	

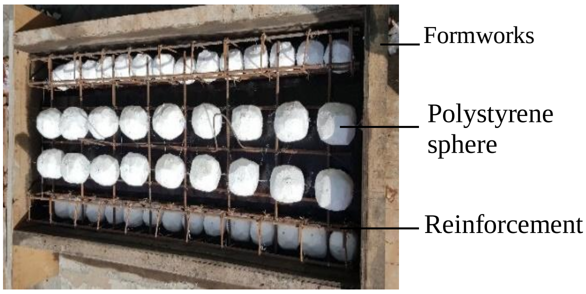

Figure 2 Details of the specimen (dimensions in mm)

METHODS AND MATERIALS

A. SPECIMENS

Four specimens were fabricated. Each specimen was made up of two beams and a slab (Figure 1). Polystyrene spheres were put in the beams and the slabs in various combinations (Table 2). The details are given in Table 3. The spacings between polystyrene spheres in the beam and the slab were 10 mm and 50 mm, respectively.

The specifications of the materials are as follows:

- Concrete: C20/25 grade, designed slump = 100 mm to 180 mm
- Reinforcements: nominal yield strength for T10 and T12 steel bars = 500 N/mm^2, nominal yield strength for R6 shear links = 250 N/mm^2

The specimens were cast in timber formworks (Figure 2). Steel reinforcements and polystyrene spheres were prepared and properly arranged in the formwork. Ready-mixed concrete was used to cast the specimens. For curing, water was sprayed on the specimens before covering them with plastic sheets. The specimens were tested after the 28th day of casting.

Table 3: Details of specimens' parts

	Beam	Slab
Dimension	175 mm x 300 mm	200 mm x 400 mm
Concrete cover	25 mm	20 mm
Reinforcements	2T10 (top), 2T12 (bottom), R8-150 (stirrup)	4T10 (longitudinal), T10-200 (transverse)
Sphere diameter	100 mm	125 mm
Sphere location	Centroid of section	40 mm from soffit
Spacing between spheres	10 mm	50 mm
Nos. of sphere	14 units x 2 rows	9 units x 2 rows

B. TEST SETUP

Each specimen was tested under a four-point load setup (Figure 3). At a clear span of 1500 mm, the specimen was simply supported. An incremental load was applied to the specimen using a hydraulic jack. The load acted on the specimen at two points, spaced at 260 mm. To measure the load and displacement, a load cell and three Linear Variable Differential Transformers (LVDT) were employed (Table 4). These devices were linked to a data logger to collect data.

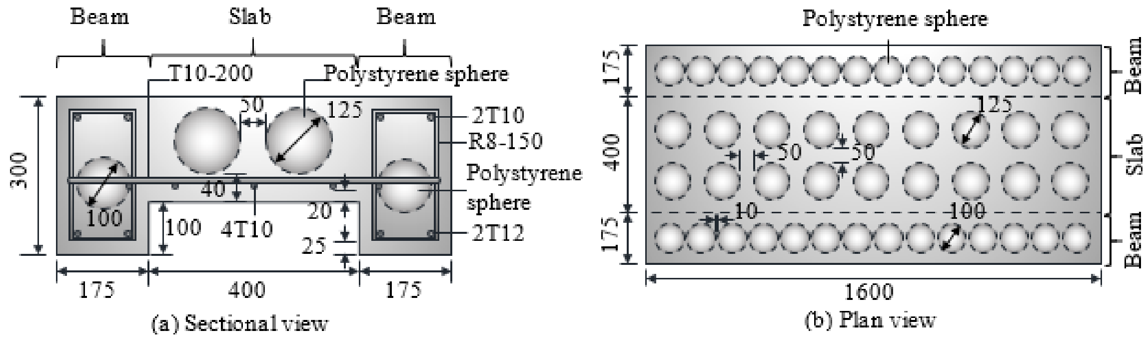

Figure 1 Details of the specimen (dimensions in mm)

Table 2: Configuration of the specimens

Specimen	Beam			Slab		
	Description	Diameter of polystyrene spheres, $d_{p,b}$ (mm)	Nos. of polystyrene spheres, $n_{p,b}$ (units)	Description	Diameter of polystyrene spheres, $d_{p,s}$ (mm)	Nos. of polystyrene spheres, $n_{p,s}$ (units)
CBS1	Solid	0	0	Solid	0	0
CBS2	Lightweight	100	28	Solid	0	0
CBS3	Solid	0	0	Lightweight	125	18
CBS4	Lightweight	100	28	Lightweight	125	18

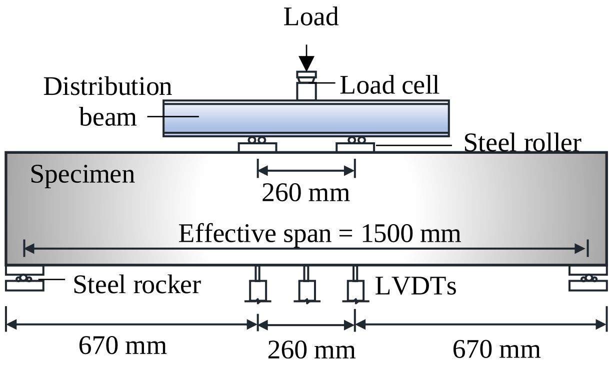

(a) Schematic setup

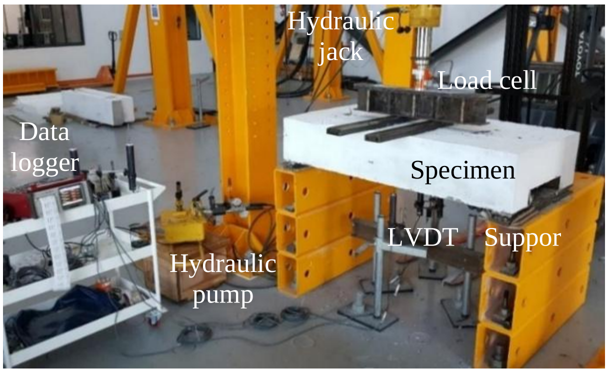

(b) Actual setup

Figure 3 Test setup

Table 4: Test equipment and instrument

Equipment / instrument	Model	Capacity	Accuracy
Hydraulic Jack	Enerpac RR-10018	933 kN load	-
Hydraulic Pump	Enerpac P-462, Two-Speed Steel Hand Pump	700 bar operating pressure	-
LVDT	TML CDP-100	100 mm stroke	± 0.01 mm
Load Cell	THL CLJ-300KNB	Capacity 300kN	± 0.1 kN
Data logger	TML TDS-630	50 Channels	0.1s measurement speed

C. TEST PROCEDURE

Before the test, a preload of roughly 10% of the specimen's estimated load capacity was applied to the specimen twice. The load was held for 5 minutes before being released. The specimen was rested for 1 minute before the next preload. This process was done as a safety measure to check the test setup and the measuring devices.

The test began by setting all readings to zero. The load was gradually raised at 5 kN or 0.5 mm intervals, whichever occurred first. The load was held for 1 minute before readings were taken. The load-displacement response and the surface cracks of the specimen were monitored during the test. The test was stopped after several consecutive drops in the load capacity.

RESULTS AND DISCUSSIONS

A. MATERIALS PROPERTIES

Table 5 and Table 6 present the material properties of the specimens. The concrete strength was higher than the designed cube strength of 25 N/mm^2. The reinforcements and shear links also met their nominal strengths of 500 N/mm^2 and 250 N/mm^2, respectively. The material quality was considered acceptable.

Table 5: Compressive strength of concrete

Specimen	Compressive Strength (N/mm^2)		Average Compressive Strength, f_{cu} (N/mm^2)
	Cube 1	Cube 2	
CBS 1	25.3	25.7	25.5
CBS 2	25.0	25.2	25.1
CBS 3	26.9	26.6	26.8
CBS 4	26.3	26.5	26.4

Table 6: Yield strength of reinforcements

Bar Diameter (mm)	Yield Strength (N/mm^2)			Average Yield Strength, f_y (N/mm^2)
	S1	S2	S3	
6	290	279	285	284.7
10	640	635	638	637.7
12	670	660	650	660.0

Note: S1, S2, and S3 represented three reinforcement bar samples

B. GEOMETRICAL PROPERTIES

Embedding polystyrene spheres in the specimen altered its geometrical properties. This is represented by the following ratios:

a. The effective area ratio, R_a, depicts the effective concrete area of the specimen's cross-section (Eqn. (1)).

$$R_a = \frac{A_c - A_p}{A_c} \quad (1)$$

Where A_c is the cross-sectional area of the entire section, mm^2, and A_p is the total cross-sectional area of polystyrene spheres in the section, mm^2.

b. The effective volume ratio, R_v, represented the effective concrete volume of the entire specimen (Eqn. (2)).

$$R_v = \frac{V_c - V_p}{V_c} \quad (2)$$

Where V_c is the volume of the entire specimen, mm^3, and V_p is the total volume of polystyrene spheres in the specimen, mm^3.

c. The effective moment of inertia ratio, R_i, is

$$R_i = \frac{I_p}{I_c} \quad (3)$$

Where I_c is the moment of inertia of the section, mm^4, and I_p is the moment of inertia of the specimen with polystyrene spheres, mm^4.

The moments of inertia of rectangular and circular sections are expressed in Eqn. (4) and Eqn. (5), respectively.

$$I = \frac{bh^3}{12} \quad (4)$$

$$I = \frac{\pi d^2}{64} \quad (5)$$

Where b is the width of a rectangular section, mm, h is the height of a rectangular section, mm, and d is the diameter of a circular section, mm.

Table 7: Ratios representing the geometrical properties of specimens

Specimen	Area of polystyrene spheres, A_p (mm^2)	Effective area ratio, R_a	Volume of polystyrene spheres, V_p (mm^3)	Effective volume ratio, R_v	Effective moment of inertia of section, I_p (mm^4)	Effective moment of inertia ratio, R_i
Ref.		Eq. 1		Eq. 2	Table 8	Eq. 3
CBS1	0	1.00	0	1.00	1,254,166,667	1.00
CBS2	15,708	0.92	14,660,766	0.95	1,244,349,190	0.99
CBS3	12,272	0.93	18,407,769	0.94	1,208,358,166	0.96
CBS4	27,980	0.85	33,068,535	0.89	1,198,540,689	0.96

**Note: beam size = 175 x 300 mm^2, slab size = 400 x 200 mm^2, Cross section area of solid specimen, A_c = 185,000 mm^2, Volume of solid specimen, V_c = 296,000,000 mm^3, Moment of inertia of solid specimen, I_c = 1,254,166,667 mm^4*

Table 8: Effective moment of inertia of specimen

Specimen	Moment of inertia of solid beam, I_b (mm^4)	Moment of inertia of solid slab, I_s (mm^4)	Moment of inertia of polystyrene sphere in beam, $I_{p,b}$ (mm^4)	Moment of inertia of polystyrene sphere in slab, $I_{p,s}$ (mm^4)	Moment of inertia of section, I_p (mm^4)	Moment of inertia of solid specimen, I_c (mm^4)
Ref.	Eq. 6	Eq. 6	Eq. 6	Eq. 6	Eq. 7	Eq. 7
CBS1	393,750,000	466,666,667	0	0	1,254,166,667	1,254,166,667
CBS2	393,750,000	466,666,667	4,908,739	0	1,244,349,190	1,254,166,667
CBS3	393,750,000	466,666,667	0	45,808,501	1,208,358,166	1,254,166,667
CBS4	393,750,000	466,666,667	4,908,739	45,808,501	1,198,540,689	1,254,166,667

The moment of inertia of a section about an axis, I_i, can be determined by using Eqn. (6).

$$I_i = I + Ad_y^2 \quad (6)$$

Where I is the local moment of inertia of a section, mm^4, A is the area of a section, mm^2, and d_y is the distance between the centroid of a section with an axis, mm.

The moment of inertia of the entire specimen, I_p, is calculated by using Eqn. (7).

$$I_p = 2(I_b - I_{p,b}) + (I_s - I_{p,s}) \quad (7)$$

Where I_b is the moment of inertia of a solid beam, mm^4, I_s is the moment of inertia of a solid slab, mm^4, $I_{p,b}$ is the moment of inertia of polystyrene sphere in the beam, mm^4, and $I_{p,s}$ is the moment of inertia of polystyrene sphere in the slab, mm^4.

These ratios (i.e., R_a, R_v, and R_i) were computed based on the following assumptions:

- The polystyrene spheres were perfectly spherical and uniform in size. In this study, the polystyrene spheres were produced manually.
- The polystyrene sphere centroids in the beams and slab were nicely aligned in a single sectional plane. This may not be the case if the spacing between the polystyrene spheres in the beam and the slab was uneven.
- The concrete was homogenous. Thus, the effective volume ratio, R_v, may also be used to represent the specimen's effective weight.
- The specimen's bending axis was located in the middle of the beam section. Therefore, the moment of inertia was calculated based on the axis.

From Table 7, the polystyrene spheres (a) occupied 8% to 15% of the specimens' cross-sections, (b) replaced 5% to 11% of the concrete volume, and (c) lowered 1% to 4% of the section's moment of inertia. Polystyrene spheres replaced a significant portion of the concrete, with no discernible reduction in the moment of inertia.

C. LOAD-DISPLACEMENT RESPONSE

The load-displacement responses of the specimens are shown in Figure 4. There were three major stages: pre-yield, post-yield, and failure stages. The pre-yield and post-yield stages represented the behaviour of the specimens before and after the yield point. The pre-yield stage can be further divided into the uncracked and cracked stages. The first crack marked the beginning of the cracked stage.

The specimens' stiffness was represented by the gradient of the load-displacement curves. The stiffness was the highest at the uncracked stage. It decreased slightly after the first crack and degraded further near the yield point. Before the yield point, the displacement was about proportionate to the load applied. The specimens reached their ultimate state as the load-displacement curve peaked.

The beams sustained more tensile strain than the slab while bending. This can be seen from the crack pattern on the specimens. Cracks formed as the concrete's strain limit was exceeded [15]. The first crack appeared at the mid-span of the beam. It began at the soffit and then propagated deeper into the beam and extended to the slab. More cracks developed as the load was increased. The cracks were mostly flexural (Figure 5). The cracks narrowed down the uncracked section and weakened the bond between the concrete and the reinforcements. This subsequently deteriorated the specimen's stiffness. Excessive cracks capped the specimens' load capacity

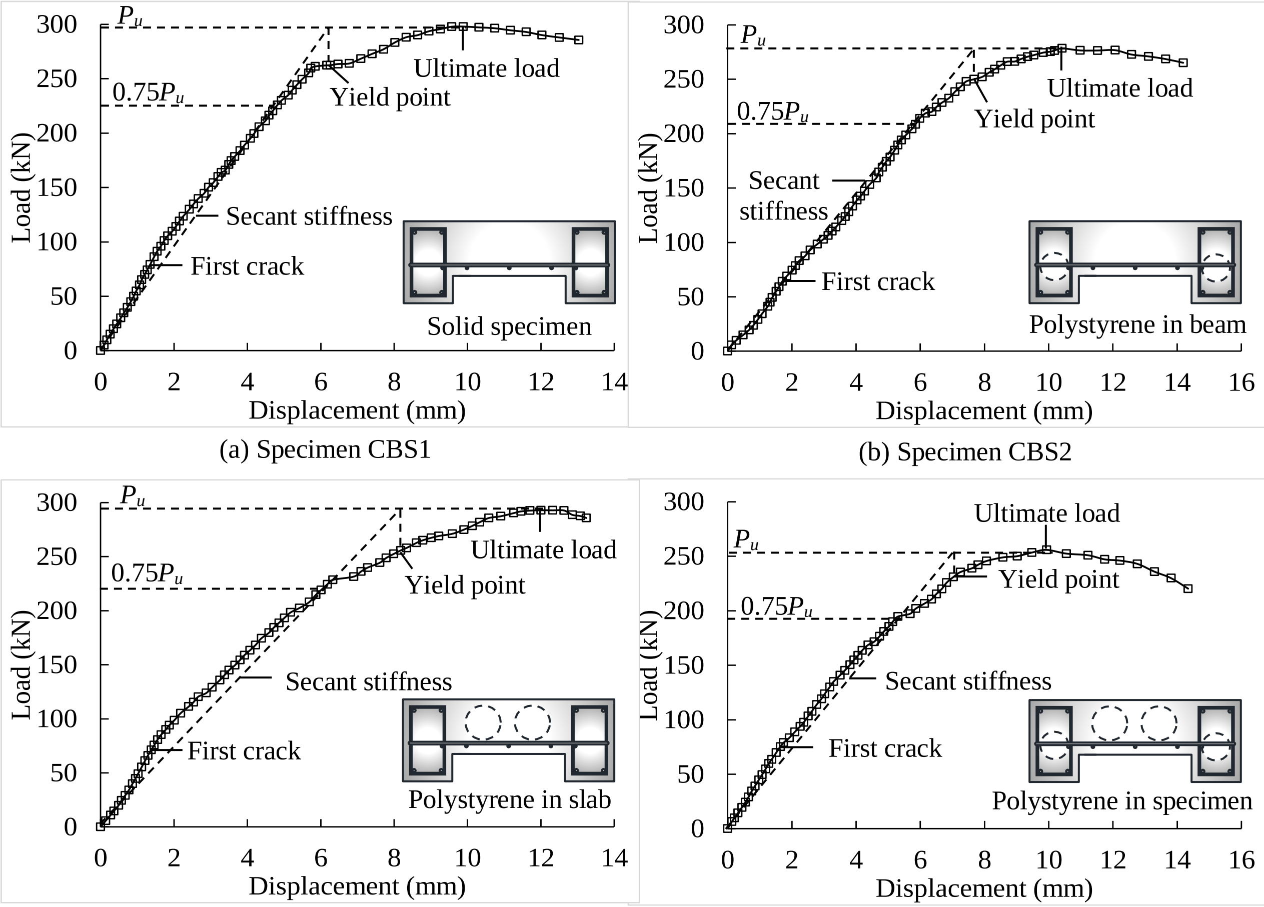

(a) Specimen CBS1
(b) Specimen CBS2
(c) Specimen CBS3
(d) Specimen CBS4

Figure 4 Load-displacement response

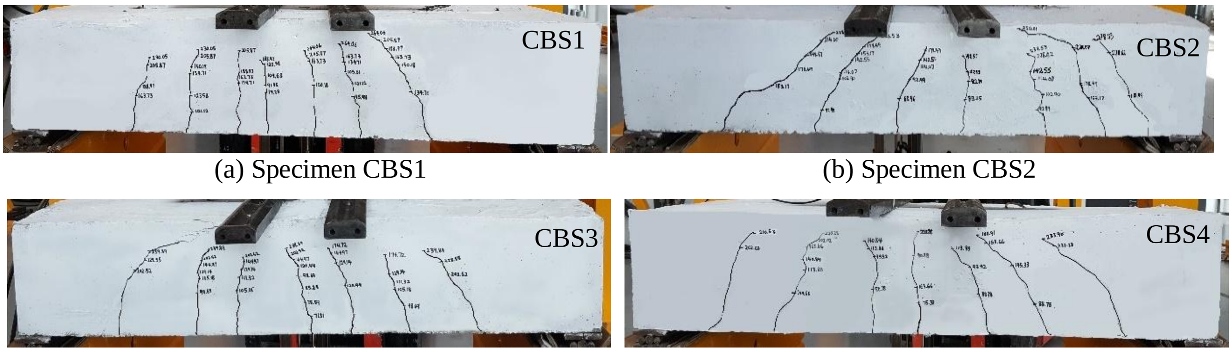

(a) Specimen CBS1
(b) Specimen CBS2
(c) Specimen CBS3
(d) Specimen CBS4

Figure 5 Crack pattern of specimens

Table 9 Test results

Specimen	First crack load, P_{cr} (kN)	First crack displacement, δ_{cr} (mm)	Secant stiffness, S (kN/mm)	Yield load, P_y (kN)	Yield displacement, δ_y (mm)	Ultimate load, P_u (kN)	Ultimate displacement, δ_u (mm)	Ductility ratio, Δ
CBS1	79.2	1.35	47.0	262.9	6.34	298.0	9.88	1.56
CBS2	69.0	1.84	35.6	251.3	7.82	278.4	10.42	1.33
CBS3	71.3	1.38	36.4	253.5	8.05	292.9	12.00	1.49
CBS4	75.4	1.64	36.8	229.0	6.95	255.9	9.93	1.43

Table 10 Description of the test results

Results	Description
First crack load, P_{cr}	The load when the first crack was noticed (Figure 5).
First crack displacement, δ_{cr}	The slab's deflection upon the first crack (Figure 4).
Secant stiffness, S_s	The stiffness representing the pre-yield response of the specimen. It was taken as the slope of the line intercepting the point $0.75P_u$ (Figure 4).
Yield point (P_y, δ_y)	The point marks the end of elastic deformation. It was determined using the $0.75P_u$ line following Park (1988) [51] (Figure 4).
Ultimate load, P_u	The largest load sustained by the specimen (Figure 4).
Ultimate displacement, δ_u	The deflection of the specimen at ultimate state (Figure 4).
Ductility ratio, Δ	An index quantifying the ductility of the specimen. It was computed by dividing the ultimate displacement, δ_u, by the yield displacement, δ_y.

The effects of polystyrene spheres can be seen by comparing CBS2, CBS3, and CBS4 to CBS1. These specimens had polystyrene spheres in various parts, whereas CBS1 was completely solid. They had a lower first crack load and stiffness than CBS1. CBS2 (i.e., lightweight beams and solid slab) was the most affected specimen of all. Its first crack load and stiffness were reduced by 13% and 24%, respectively. The polystyrene spheres removed the concrete, which subsequently reduced the specimens' ability to resist deformation. This accelerated the tensile strain and quickly initiated the crack.

Among the specimens, CBS1 was the strongest. This was followed by CBS3, CBS2, and CBS4. This can be observed from the yield and ultimate loads of the specimens (Table 9). As a solid section, CBS1 had the greatest moment of inertia (Table 8). This improved its load-bearing capacity. Conversely, CBS4 (i.e., lightweight beams and slab) had the largest area occupied by polystyrene spheres (Ra = 0.85, Table 7). The moment of inertia was consequently reduced. As a result, it had the lowest yield and ultimate load of all.

CBS2 (i.e., lightweight beams and solid slab) was weaker than CBS3 (i.e., solid beams and lightweight slab) despite having a greater moment of inertia. Its polystyrene spheres were embedded in the beams, whereas CBS3's were in the slab. According to [11], the beams with embedded polystyrene spheres were less effective than the slabs. This was also due to CBS2's smaller spacing between polystyrene spheres than CBS3. This spacing formed the ribs in the specimen. They helped distribute stress in the specimen [33]. The smaller ribs in CBS2 were ineffective at spreading stress from the high-stress regions. This, to some extent, affected the specimen's load capacity.

FEASIBILITY EVALUATION

The specimens were evaluated for feasibility in various aspects. The preferred states of specimens are outlined as follows:

a. C1: The cocrete volume governs its weight, whereas the moment of inertia influences bending resistance. The weight decrease imposed by the polystyrene spheres should, ideally, have no substantial effect on the bending resistance. On this basis, the effective moment of inertia ratio, R_i, should be greater than the effective volume ratio, R_v. Thus, the geometry ratio, R_g, should be greater than 1.0.
$$R_g = \frac{R_i}{R_v} > 1.0 \quad (8)$$
Where, R_i is the effective moment of inertia ratio of the specimen, and R_v is the effective volume ratio of the specimen.

b. C2: The polystyrene spheres should increase the material's efficiency in the specimen. The specimens should have a higher strength per unit of concrete than the solid specimen. Hence, the efficiency ratio, R_e, should be at least 1.0.
$$R_e = \frac{E_i}{E_c} \geq 1.0 \quad (9)$$
Where E_i is the strength per unit concrete volume of the specimen, kN/mm^3, E_c is the strength per unit concrete volume of the solid specimen, kN/mm^3.

c. C3: The specimens with polystyrene spheres should have a comparable strength to the solid specimen. Their load capabilities should be higher than the solid specimen's. Therefore, the strength ratio, R_s, should be greater than 1.0.
$$R_s = \frac{P_{u,i}}{P_{u,c}} \geq 1.0 \quad (10)$$
Where $P_{u,i}$ is the ultimate load of the specimen, kN, and $P_{u,c}$ is the ultimate load of the solid specimen, kN.

d. C4: The yield point defines the service load of a specimen. The service load should not be too low compared with the load capacity. It governs the specimen's design strength. To minimised the non-usable strength, the serviceability ratio, R_{sv}, should be at least 0.75 [52], [53].
$$R_{sv} = \frac{P_y}{P_u} \geq 0.75 \quad (11)$$
Where P_y is the yield load of the specimen, kN, and P_u is the ultimate load of the solid specimen, kN.

e. C5: The specimen should exhibit ductile behaviour for survival purposes. For structural application in low to moderate seismic zones, the ductility ratio, Δ, should be at least 4.0 [4], [52], [54] - [56].
$$\Delta = \frac{\delta_u}{\delta_y} \geq 4.0 \quad (12)$$
Where δ_u is the ultimate displacement of the specimen, mm, and δ_y is the yield displacement of the specimen, mm

Table 11 evaluates the specimens against Criteria C1 to C5. None of the specimens met all the requirements. CBS1 performed the best overall. It fulfilled four out of five criteria. Its ductility was inadequate. However, this specimen was entirely solid, and it offered no weight reduction.

CBS3 was the second-best option. It met three out of the five criteria. The specimen had polystyrene spheres embedded in slabs. Concrete was the most efficiently used. The efficiency ratio, R_e, was the highest of all. Its strength ratio, R_s, was the closest to 1.0. Although the ductility ratio was slightly lower than the solid specimen, CBS3's ultimate displacement was the largest of all (Table 9). Nevertheless, the ductility was still insufficient.

CBS2 and CBS4 performed poorly. They only met two of the criteria. Polystyrene spheres reduced the weight and

Table 11 Feasibility evaluation

Specimen	C1		C2				C3		C4		C5		
	Geometry ratio, R_g		Volume specimen, V_i (mm^3)	Strength per unit concrete volume, E_i	Efficiency ratio, R_e		Strength ratio, R_s		Serviceability ratio, R_{sv}		Ductility ratio, R_d		Score*[2]
Equations	(8)				(9)		(10)		(11)		(12)		
Requirements		≥1				≥1		≥1		≥0.75		≥1	
CBS1	1.00	√	296,000,000	0.00101	1.00	√	1.00	√	0.88	√	1.56	X	4/5
CBS2	1.04	√	281,339,234	0.00099	0.98	X	0.93	X	0.90	√	1.33	X	2/5
CBS3	1.02	√	277,592,231	0.00106	1.05	√	0.98	X	0.87	√	1.49	X	3/5
CBS4	1.08	√	262,931,465	0.00097	0.96	X	0.86	X	0.89	√	1.43	X	2/5

Note: [1]Volume of polystyrene spheres, V_p, Effective volume ratio, R_v, and Effective moment of inertia ratio, R_i, refer to Table 7; Ultimate load, P_u, yield load, P_y, and ductility ratio, Δ, refer to Table 9.
[2]Nos. of criteria met out of five.

load capacity of CBS4 by 11% and 14%, respectively. The efficiency ratio, R_e, was less than 1.0. Polystyrene spheres were ineffective in the beams of CBS2. The specimen had an efficiency ratio of less than 1.0. It was also 7% weaker than the solid specimen.

CONCLUSIONS

In this study, polystyrene spheres were used to replace 5% to 11% of the concrete in an RC system comprising beams and slab. Polystyrene spheres worked well in the slab but not in the beams. Embedding polystyrene spheres in the slab increased its effectiveness by 5%. When polystyrene spheres were placed in the beams or in the beams and slab, the performance dropped. The material's efficiency declined by 2% to 4%, and the load capacity decreased by 7% to 14%.

The specimens' feasibility was evaluated using five criteria. None of the specimens met all of the requirements. The specimens lacked ductility. Despite its superior efficiency, embedding polystyrene spheres in the slab was the second-best option after the solid specimen. Polystyrene spheres appeared to inevitably reduce the specimen’s strength in the current design. The shape and dimension of the polystyrene in the specimen could be modified to see if the structural performance can be further improved. The slab's span could be expanded to further improve system efficiency.

ACKNOWLEDGMENTS

This research work was funded by the Research Grants of University of Technology Sarawak UCTS/ RESEARCH/2/2018/02.

REFERENCES

[1] [M. U. Hanif, Z. Ibrahim, K. Ghaedi, H. Hashim, and A. Javanmardi, "Damage assessment of reinforced concrete structures using a model-based nonlinear approach – A comprehensive review," Construction and Building Materials, vol. 192, pp. 846-865, 2018.
[2] H. S. Dweik, M. M. Ziara, and M. S. Hadidoun, "Enhancing concrete strength and thermal insulation using thermoset plastic waste," International Journal of Polymeric Materials and Polymeric Biomaterials, vol. 57, pp. 635-656, 2008.
[3] J. H. Ling, J. W. Lau, and Y. T. Lim, "Structural behaviour of reinforced concrete beam with embedded polystyrene spheres," Civil and Sustainable Urban Engineering, vol. 3, pp. 25-39, 2023.
[4] J. W. Lau, J. H. Ling, and Y. T. Lim, "Feasibility study of reinforced concrete beam with embedded polystyrene spheres under incremental flexural load," Borneo Journal of Science & Technology, vol. 2, pp. 11-26, 2020.
[5] L. Ragavi, "Behaviour of reinforced concrete hollow beams under monotonic loading," World Journal of Technology, Engineering and Research vol. 2, pp. 127-136, 2017.
[6] A. J. H. Alshimmeri and H. N. G. Al-Maliki, "Structural behavior of reinforced concrete hollow beams under partial uniformly distributed load," Journal of Engineering, vol. 20, pp. 130-145, 2014.
[7] T. S. Al-Gasham, A. N. Hilo, and M. A. Alawsi, "Structural behavior of reinforced concrete one-way slabs voided by polystyrene balls," Case Studies in Construction Materials, vol. 11, pp. 1-13, 2019.
[8] S. Inoue and N. Egawa, "Flexural and shear behaviour of reinforced concrete hollow beams under reversed cyclic loads," presented at the Eleventh World Conference on Earthquake Engineering, 1996.
[9] Y. T. Lim and J. H. Ling, "Incorporating lightweight materials in reinforced concrete beams and slabs – A review," Borneo Journal of Sciences and Technology, vol. 1, pp. 16-26, 2019.
[10] Y. T. Lim, J. H. Ling, J. W. Lau, and T. T. L. Danson, "Performance of reinforced concrete beam with polystyrene blocks at various regions," Journal of Science and Applied Engineering, vol. 3, pp. 62-71, 2021.
[11] S. Soji and P. Anima, "Experimental and analytical investigation on partial replacement of concrete in the tension zone," International Journal of Engineering Research and General Science, vol. 4, pp. 23-32, 2016.
[12] J. W. Lau, "Behaviour of lightweight reinforced concrete beam and slab system with embedded polystyrene spheres under flexural load," Master, School of Engineering and Technology, University College of Technology Sarawak, 2021.
[13] Y. T. Lim, J. H. Ling, J. W. Lau, and A. Y. M. Yik, "Experimental study on the flexural behavior of reinforced polystyrene blocks in concrete beams," Journal of the Civil Engineering Forum, vol. 7, pp. 197-208, 2021.
[14] J. H. Chung, J. H. Park, H. K. Choi, S. C. LEE, and C. S. CHOI, "An analytical study on the impact of hollow shapes in bi-axial hollow slabs," in Proceedings of

Fracture Mechanics of Concrete and Concrete Structures - High Performance, Fiber Reinforced Concrete, Special Loadings and Structural Applications (FraMCoS-7), 2010.

[15] J. H. Ling, J. T. S. Ngu, Y. T. Lim, W. K. Leong, and H. T. Sia, "Experimental study of RC hollow beams with embedded PVC pipes," Journal of Advanced Civil and Environmental Engineering, vol. 5, pp. 11-23, 2022.

[16] J. H. Ling, L. L. Chan, W. K. Leong, and H. T. Sia, "The development of finite element model to investigate the structural performance of reinforced concrete hollow beams," Journal of the Civil Engineering Forum, vol. 6, pp. 171-182, 2020.

[17] H. Mohd Noh, N. L. I. Azwani Mohamad, and R. Bangau, "Performance of hollow reinforced concrete beam in structural member," Journal of Mechanical Engineering vol. 17, pp. 1-11, 2020.

[18] J. Joy and R. Rajeev, "Effect of reinforced concrete beam with hollow neutral axis " International Journal for Scientific Research & Development, vol. 2, pp. 341-348, 2014.

[19] N. Parthiban and M. Neelamegam, "Flexural behavior of reinforced concrete beam with hollow core in shear section," International Research Journal of Engineering and Technology, vol. 4, pp. 2263-2274, 2017.

[20] T. S. S. Al-Gasham, "Reinforced concrete moderate deep beams with embedded PVC pipes," Wasit Journal of Engineering Science vol. 3, pp. 19-28, 2015.

[21] N. A. Idris, H. Mohd Noh, N. L. I. Azwani Mohamad, and R. Bangau, "Reinforced concrete by using the rectangular shape of voided beam," Journal of Mechanical Engineering vol. 9, pp. 179-190, 2020.

[22] G. Balaji and R. Vetturayasudharsanan, "Experimental investigation on flexural behaviour of RC hollow beams," Materialstoday: Proceeding, vol. 21, pp. 351-356, 2020.

[23] N. Z. Hassan, H. M. Ismael, and A. M. Salman, "Study behavior of hollow reinforced concrete beams," International Journal of Current Engineering and Technology, vol. 8, pp. 1640-1651, 2018.

[24] B. G. Bhade and S. M. Barelikar, "An experimental study on two way bubble deck slab with spherical hollow balls," International Journal of Recent Scientific Research, vol. 7, pp. 11621-11626, 2016.

[25] S. Ali and M. Kumar, "Analytical study of conventional slab and bubble deck slab under various support and loading conditions using Ansys Workbench 14.0," International Research Journal of Engineering and Technology, vol. 4, pp. 1467-1472, 2017.

[26] A. A. Alfeehan, H. I. Abdulkareem, and S. H. Mutashar, "Flexural behavior of sustainable reactive powder concrete bubbled slab flooring elements," Challenge Journal of Structural Mechanics vol. 3, pp. 81-89, 2017.

[27] M. R. K. M. Al-Badkubi, "Finite element study on ultimate shear capacity of voided reinforced concrete beams," in 2nd International Conference on Engineering Technology and their Applications 2019-IICET2019, 2019.

[28] A. E. Ajeel, T. A. Qaseem, and S. R. Rasheed, "Structural behavior of voided reinforced concrete beams under combined moments," Civil and Environmental Research vol. 10, pp. 17-24, 2018.

[29] N. Mohamad, W. I. Goh, A. A. A. Samad, A. Lockman, and A. Alalwani, "Structural behaviour of beam with HDPE plastic balls subjected to flexural load," Materials Science Forum vol. 889, pp. 270-274, 2017.

[30] R. R. Patel, "Flexural behavior and strength of doubly-reinforced concrete beams with hollow plastic spheres," Master of Science (Civil Engineering), Old Dominion University, 2018.

[31] M. R. K. M. Al-Badkubi, "Finite element study on flexural behavior of voided concrete beams," International Journal of Civil Engineering and Technology, vol. 9, pp. 123-138, 2018.

[32] J. H. Chung, H. K. Choi, S. C. Lee, and C. S. Choi, "Shear capacity of biaxial hollow slab with donut type hollow sphere," Procedia Engineering, vol. 14, pp. 2219–2222, 2011.

[33] H. T. Nimnim and Z. M. J. Zain Alabdeen, "Structural behavior of voided normal and high strength reinforced concrete slabs," Kufa Journal of Engineering, vol. 10, pp. 1-11, 2019.

[34] N. Oukaili and H. H. Yasseen, "Experimental investigations on the strength and serviceability of biaxial hollow concrete slabs," Journal of Engineering vol. 22, pp. 36-54, 2016.

[35] A. Raza and M. E. Ahmad, "Comparison of voided and solid reinforced concrete slabs," in Proceedings of the 1st International Conference on Recent Advances in Civil and Earthquake Engineering, Peshawar, Pakistan, 2021.

[36] M. Schnellenbach-Held and K. Pfeffer, "Punching behavior of biaxial hollow slabs," Cement and Concrete Composites, vol. 24, pp. 551-556, 2002.

[37] A. M. Ibrahim, M. A. Ismael, and H. A. S. Abdul Hussein, "The effect of balls shapes and spacing on structural behaviour of reinforced concrete bubbled slabs," Journal of Engineering and Sustainable Development, vol. 23, 2019.

[38] I. Mathew and S. M. Varghese, "Experimental study on partial replacement of concrete in and below neutral axis of beam," International Journal of Innovative Research in Technology, vol. 3, pp. 188-192, 2016.

[39] S. Sariman and A. R. Nurdin, "Flexural behavior of t shaped reinforced concrete hollow beam with plastic bottle waste," International Journal of Civil Engineering and Technology, vol. 9, pp. 534-543, 2018.

[40] B. t. jose and D. Sasi, "Comparative study on partial replacement of concrete below neutral axis of beam using seeding trays and polythene balls," International Journal of Innovative Science, Engineering & Technology, vol. 5, pp. 172-177, 2018.

[41] A. M. Ibrahim, N. K. Ali, and W. D. Salman, "Flexural capacities of reinforced concrete two-way bubbledeck slabs of plastic spherical voids," Diyala Journal of Engineering Sciences, vol. 6, pp. 9-20, 2013.

[42] C. H. Lee, I. Mansouri, E. Kim, J. Ryu, and W. T. Woo, "Experimental analysis of one-way composite steel deck slabs voided by circular paper tubes: Shear

strength and moment–shear interaction," Engineering Structures, vol. 182, pp. 227-240, 2019.
[43] P. Sivaneshan and S. Harishankar, "Experimental study on voided reinforced concrete beams with polythene balls," IOP Conf. Series: Earth and Environmental Science vol. 80, pp. 1-8, 2017.
[44] A. F. Izzat, J. A. Farhan, and N. M. Allawi, "Behaviour and strength of one way reinforced concrete slabs with cavities," 2014.
[45] A. Y. M. Yik and J. H. Ling, "Experimental study on voided slab subjected to flexural load," Borneo Journal of Sciences and Technology, vol. 2, pp. 27-31, 2020.
[46] D. T. L. Tan and J. H. Ling, "Flexural behaviour of reinforced concrete beam embedded with different alignment of polystyrene," Borneo Journal of Sciences and Technology, vol. 2, pp. 13-18, 2020.
[47] S. Manikandan, S. Dharmar, and S. Robertravi, "Experimental study on flexural behaviour of reinforced concrete hollow core sandwich beam," International Journal of Advance Research in Science and Engineering, vol. 4, pp. 937-946, 2015.
[48] H. A. Jabir, M. Jasim, and T. S. Al-Gasham, "Conventional and bubble slab strips under limited repeated loads: A comparative experimental study," Case Studies in Construction Materials, 2021.
[49] Z. M. Jaini, H. B. Koh, S. N. Mokhatar, I. Mat, H. Hazmi, and N. H. Hashim, "Structural behaviour of short-span reinforced concrete beams with foamed concrete infill," ARPN Journal of Engineering and Applied Sciences, vol. 11, pp. 9820-9824, 2016.
[50] U. N. Kumbhar and H. S. Jadhav, "Flexural behaviour of reinforced concrete hollow beam with polypropylene plastic sheet infill," International Research Journal of Engineering and Technology, vol. 5, p. 1517, 2018.
[51] R. Park, "Ductility evaluation from laboratory and analytical testing," in The 9th world conference on earthquake engineering, Tokyo-Kyoto, Japan, 1988, pp. 605-616.
[52] J. H. Ling, A. B. Abd. Rahman, I. S. Ibrahim, and Z. Abdul Hamid, "An experimental study of welded bar sleeve wall panel connection under tensile, shear, and flexural loads," International Journal of Concrete Structures and Materials, vol. 11, pp. 525–540, September 12 2017.
[53] J. H. Ling, A. B. Abd. Rahman, and I. S. Ibrahim, "Deformation behavior of grouted sleeve wall connector under shear load in precast process of concrete wall," Indonesian Journal of Computing, Engineering, and Design, vol. 4, pp. 1-14, 2022.
[54] K. A. Soudki, "Behaviour of horizontal connections for precast concrete load-bearing shear wall panels subjected to reversed cyclic deformations," PhD, Structural Engineering Division, Department of Civil & Geological Engineering, University of Manitoba, Winnipeg, Manitoba, 1994.
[55] J. H. Ling, J. H. Lim, and A. B. Abd. Rahman, "Behaviour of precast concrete beam-to-column connection with shs hidden corbel subjected to monotonic load," Journal of the Civil Engineering Forum, vol. 7, pp. 223-238, 2021.
[56] J. H. Ling, A. B. Abd. Rahman, and I. S. Ibrahim, "Feasibility study of grouted splice connector under tensile load," Construction and Building Materials, vol. 50, pp. 530-539, 2014.